QUANTUM CHEMICAL INVESTIGATION OF THE STRUCTURE AND NMR PROPERTIES OF SOME IMIDAZOLE DERIVATIVES WITH ANTIPROLIFERATIVE ACTIVITY

M. Georgieva[1*], L. Andonova[1], G. Momekov[2], B. Zlatkov[1], Al. Zlatkov[1]

[1]Department of Pharmaceutical Chemistry, Medical University of Sofia, Faculty of Pharmacy, 2 Dunav Street, 1000 Sofia, Bulgaria

[2]Department of Pharmacology and Toxicology, Medical University of Sofia, Faculty of Pharmacy, 2 Dunav Street, 1000 Sofia, Bulgaria

Abstract. Correlations between experimental chemical shifts and GIAO-calculated isotropic shielding constants of hydrogen and carbon atoms were obtained for a series of imidazole derivatives with antiproloferative activity, in order to assess the performance of NMR spectral calculations, using both HF and DFT-B3LYP level of theory with different basis sets. The influence of the choice of the method and the basis set on the chemical shift was investigated. The theoretical values were compared with the experimental data. The experimental shifts for carbons are in better agreement with the HF/6-311 G(d) and B3LYP/6-31 G(d) calculations, whereas for protons the differences are almost negligible. The calculated root mean square values for 1H shifts indicate that the 6-311+G(2d,p) basis set provides better fit for chemical shifts than the other basis sets. The obtained b values differ with statistical significance from zero ($P < 0.001$), which on the linear model used is adequate and correctly describes the dependence between the experimental and the calculated values of the corresponding chemical shifts. The analysis of the obtained pharmacological data for the newly synthesized imidazole derivatives shows that the target structures possess antiproliferative activity and they may be recognised as leading structures for future development of new anti-neoplastic agents.

Key Words: DFT, HF, GIAO, ^{1}H-, ^{13}C NMR, imidazole derivatives, structure-correlation analysis, antiproliferative activity

Introduction

Imidazole is a five-membered heterocyclic system with three carbon and two nitrogen atoms at 1- and 3-position. The imidazole core is forecasted to be a good pharmacophore and represents an important synthetic precursor in new drug discovery. It is a common moiety in a large number of natural products and pharmacologically active compounds [1–4]. Some of the substituted imidazole derivatives have emerged as multifunctional "drug-biomarker monitors" with importance in treatment of tumors, monitoring hypoxia [5, 6] and safer imaging contrast agents to monitor the therapeutic process. Imidazole nucleus is incorporated into main structure of many biologically important molecules, among which the most important are the amino acid histidine and the purines, which comprise many of the important bases in nucleic acids, vitamin B12 and biotin. Also the role of imidazole derivatives as precursors in the biosynthesis of purine alkaloids is well known [7, 8].

On the other hand in aqueous alkaline solution the methylxanthines Caffeine, Theophylline and Etofylline undergo a hydrolytic cleavage of the pyrimidine ring at 1,2 positions to give corresponding N,1-dimethyl-4-(methylamino)-1H-imidazole-5-carboxamide (Caffeidine), N-methyl-4-(methylamino)-1H-imidazole-5-carboxamide (Theophyllidine) and 1-(2-hydroxyethyl)-N-methyl-4-(methylamino)-1H-imidazole-5-carboxamide (Etofyllidine) [9 – 12]. This hydrolytic pathway may be concerned as an appropriate method for synthesis of substituted 1H-imidazole-5-carboxamide derivatives. However, to our knowledge, there is no information about the pharmacological properties of above cited imidazole derivatives as well as any investigations on their molecular structure.

The biological activity of the compounds is supposed to depend on their molecular structure. NMR spectroscopy has been proven to be an exceptional method to prove molecular structure. *Ab initio* and DFT calculation of NMR shielding at very accurate levels of approximation are available in literature

[13]. Comparison between experimental and theoretical spectra is a useful tool to make correct assignments and collaborates to getting a better knowledge of the relationship between chemical shifts and molecular conformations [14]. One of the widely used methods to calculate chemical shifts is GIAO (gauge independent or invariant or including atomic orbital). This approach [15] introduces a local gauge origin for each atomic orbital and is known to give satisfactory chemical shifts for small- and medium-size systems [14], yielding data comparable with those of the experiment. It was suggested that the combination of high-level *ab initio* optimized geometries, theoretically computed NMR chemical shifts, and experimental NMR data provides a tool that can be routinely applied for structural elucidation and characterization of new compounds [16]. On the other hand, it is clear that a good correlation between the experimental and theoretical properties of the molecules will be achieved when the theoretically considered structure follows the real one with a good approximation.

Keeping in mind the biological importance of the substituted imidazoles, we present an investigation on molecular structure and NMR behavior of three substituted ^{1}H-imidazole-5-carboxamide derivatives. The DFT and *ab initio* methods were applied to calculate the theoretical isotropic ^{1}H and ^{13}C chemical shifts. The calculated chemical shifts are then compared with the experimental values. Antiproliferative activity of the studied compounds was also evaluated.

Materials and methods

Spectra

The NMR spectra were measured on a Bruker DRX250 (250 MHz) spectrometer (Germany) using D_2O as solvent and chemical shifts were expressed as δ values in ppm against TMS as an internal standard; standard abbreviations are used.

Computational details

All names were generated, using structure-to-name and name-to-structure algorithms included with ChemBioDraw Ultra 11.0 (CambridgeSoft) [17].

The *ab initio* calculations (Hartree-Fock (HF)) and density functional theory (DFT) calculations reported herein were obtained using GAUSSIAN 03W, ver. 6.1 [18] and GausView molecular visualization program [19] on a computer with Intel Pentium dual-core CPU E6500 at 2.93 GHz and 4 GB RAM.

The energetically preferred geometries were calculated by energy minimization using AM1 Hamiltonian [20]. All molecular structures of the title compounds in ground state (in vaccuo) are optimised applying HF and B3LYP methods with 6-31G (d), 6-311G(d) and 6-311+G(2d,p) basis sets. 1H and 13C isotropic magnetic shielding tensors were calculated with GIAO approach using the same level of theory. Then the predicted ^{1}H and ^{13}C chemical shifts were derived by subtracting calculated isotropic magnetic shielding (IMS) from the IMS value of TMS, given in Table 1.

Table 1. *The isotropic magnetic shielding tensors (in ppm) of TMS for 13C and 1H calculated at GIAO model with different basis sets [21].*

Method/Basis set	^{13}C	^{1}H
HF/6-31G(d)	199.9921	32.5968
HF/6-311G(d)	194.5082	32.5787
HF/6-311+G(2d,p)	192.5973	32.0730
B3LYP/6-31G(d)	189.7026	32.1836
B3LYP/6-311G(d)	184.2796	32.2899
B3LYP/6-311+G(2d,p)	182.4656	31.8221

The predicted chemical shift values were calculated using the following equation:

$$\delta_{pred.} = \sigma_{IMS_{TMS}} - \sigma_{IMS_{calc.}}$$

Linear correlation analyses were carried out using Origin 6.1 program. The quality of each correlation was judged with r value, the Pearson correlation coefficient [22], as well as coefficient of determination (r^2, RMSError).

The numbering systems of the compounds for which calculations were carried out, are presented on Fig. 1.

Drugs, chemicals and reagents.

Formic acid, 2-propanol and L-glutamine were purchased from AppliChem GmbH, Darmstadt, Germany. Fetal calf serum (FCS) and RPMI 1640 medium were purchased from Sigma – Aldrich Co., USA. The tetrazolium salt 3-(4,5-dimethylthi¬azol-2-yl)-2,5-diphenyl tetrazolium bromide (MTT) was supplied from Merck Co., Germany. The referent antineoplastic drug melphalan was used as a commercially available pharmaceutical grade substance.

Cell lines and culture conditions.

The study was carried out with the following cell lines: BV-173 (ACC 20) – human B-cell precur-

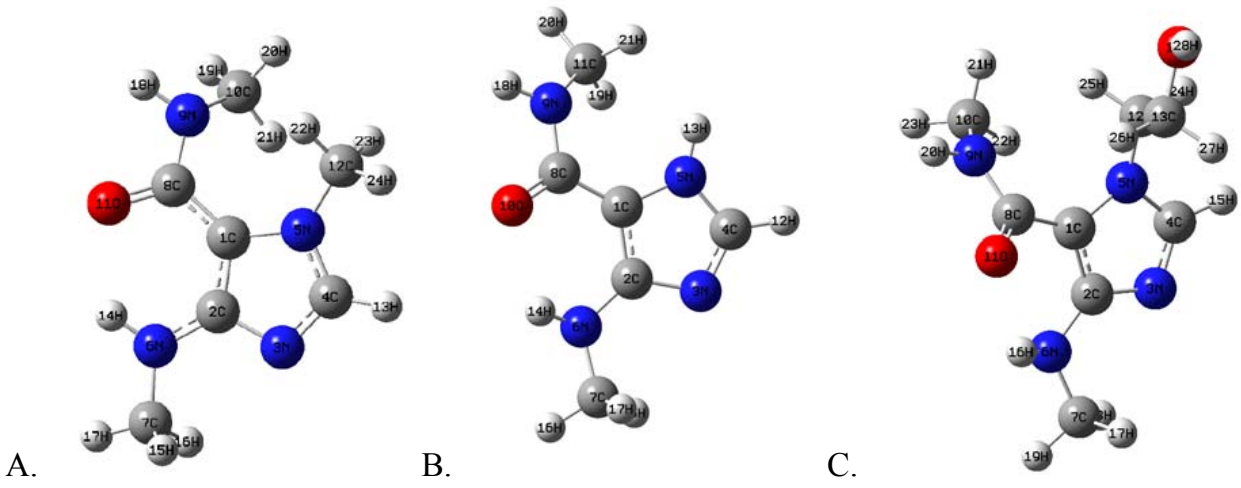

Fig 1. The numeration scheme for: A – N,1-dimethyl-4-(methylamino)-1H-imidazole-5-carboxamide (1, Caffeidine), B – N-methyl-4-(methyl-amino)-1H-imidazole-5-carboxamide (2, Theophyllidine), C – 1-(2-hydroxyethyl)-N-methyl-4-(methylamino)-1H-imidazole-5-carboxamide (3, Etofyllidine).

sor leukemia, originally described to be established from the peripheral blood of a 45-year-old man with chronic myeloid leukemia (CML) in blast crisis in 1980; contains the t(9;22) leading to BCR-ABL1 e13-a2 (b2-a2) fusion gene; KG-1 (ATCC® CCL-246™) – macrophage cell type, established from the bone marrow of a 59 years old Caucasian man with acute myelogenous leukemia.

The cell lines were obtained from the German Collection of Microorganisms and Cell Cultures (DSMZ GmbH, Braunschweig, Germany). They were cultured under standard conditions - RPMI-1640 liquid medium supplemented with 10% fetal bovine serum (FBS) and 2 mM L-glutamine, in cell culture flasks, housed at 37°C in an incubator "BB 16-Function Line" Heraeus (Kendro, Hanau, Germany) with humidified atmosphere and 5% CO_2. Cell cultures were maintained in logarithmic growth phase by supplementation with fresh medium two or three times weekly.

Cytotoxicity assessment (MTT-dye reduction assay).

The cell viability after exposure to the tested compounds was assessed using the MTT-dye reduction assay, based on the biotransformation of the yellow dye 3-(4,5-dimethylthi¬azol-2-yl)-2,5-diphenyl tetrazolium bromide to a violet formazan product via the mitochondrial succinate dehydrogenase in viable cells. The procedure was carried out as described elsewhere [23], with some modifications [24]. Exponentially growing cells were seeded in 96-well flat-bottomed microplates (100 µl/well) at a density of 1x105 cells per ml and after a 24 h incubation period at 37°C they were treated with graded concentrations of the extract (or its fractions) for 72h. For each concentration a set of 8 wells was used. After the exposure period 10µl MTT solution (10mg/ml in PBS) aliquots were added to each well. The microplates were further incubated for 4h at 37°C and the MTT-formazan crystals formed were dissolved through addition of 100 µl/well 5% formic acid in 2-propanol. The MTT-formazan absorption was determined using a microprocessor controlled microplate reader (Labexim LMR-1) at 580 nm.

Bioassay data processing and statistics.

The cell survival data were normalized as percentage of the untreated control (set as 100% viability), were fitted to sigmoidal dose response curves and the corresponding IC50 values (concentrations causing 50% suppression of cellular viability) were calculated using non-linear regression analysis (GraphPad Prizm Software for PC). The statistical processing of biological data included the Student's t-test whereby values of $p \leq 0.05$ were considered as statistically significant.

Results and discussion

The geometries of the structures were optimized at adopted C1 point group symmetry, since these molecular structures include methyl groups and short side chains, bounded to the imidazole ring and are non-planar. The optimized structures of investigated compounds are presented in Fig. 1. The geometrical parameters (bond lengths, bond angles and torsion

angles) of the compounds calculated at B3LYP/6–31G(d,p) level of theory are presented in Table 2. The results from B3LYP/6-311+G(2d,p) calculation are quite similar to the presented.

The accurate, experimental geometrical parameters for studied compounds are not available because of an absence of crystallographic data. Theoretical, energy-optimised geometries are similar to each other. The selected calculated bond lengths and angles of imidazole residue in all of the investigated molecules, have been compared with structural parameters of the crystal structure of imidazole [25] (Table 2), in accordance with the used atom numbering (Fig. 1). The bond lengths and bond angles of the imidazole fragment in the studied molecules are in good agreement with the crystallographic data for imidazole. The theoretical and the experimental values differ by 0.02 Å to 0.07 Å and 0.2º to 1.7º. This deviation may be due to the fact that the theoretical calculations apply to a single molecule in a gas phase, whereas the experimental results apply to a molecule in a solid state. On the other hand the experimental values are for unsubstituted imidazole. The lengths of the methyl C–H bonds in methyl groups vary from 1.087 Å to 1.095 Å. However, the calculated values were found to be in a good agreement with those reported for caffeine structure by Poltev [26] (obtained by MP2/6-31G(d,p) calculations) and Egawa [27] (obtained by MP2/6-31G** and B3LYP/6-31G** calculations). The imidazole ring and side chains connected to C1 and C2, except the hydrogens of the methyl groups, in all compounds are essentially coplanar, but in **3** there is small deviations from the plane probably due to the influence of the 2-hydroxyethyl substituent at N5 which also deviates from the plane.

The calculations of ^{1}H and ^{13}C isotropic magnetic shielding tensors produce absolute shielding values. In order to obtain the results comparable with the experimental data tetramethylsilane (TMS, (CH3)4Si) was used as reference. The calculated absolute shielding values are converted to relative chemical shifts by subtraction from the shielding value for TMS, obtained at the same level of theory used in the calculation of absolute shieldings of the compounds. The experimental and the theoretical results, along with the differences for each compound are presented in Tables 3-5.

A least square fit of all data as presented on Fig. 2, shows a strong linear relationship. The following correlation:

$$\delta_{calc} = a + b\delta_{exp}$$

was established and details are summarized in Table 6.

Table 2. *Selected bond lengths (A°), bond angles (°) and torsion angles (°).*

	1	**2**	**3**	**Imidazole**[23]
C1 - C2	1.396	1.393	1.386	1.358
C2 - N3	1.426	1.427	1.411	1.378
N3 - C4	1.350	1.354	1.356	1.326
C4 - N5	1.382	1.376	1.394	1.349
C1 - N5	1.436	1.431	1.413	1.369
C1 - C8	1.449	1.449	1.453	-
C8 - N9	1.388	1.385	1.382	-
C2 - N6	1.381	1.379	1.416	-
C4 – H13/12/15	1.085	1.084	1.082	1.09
N5 – H13	-	1.012	-	1.05
N5 - C4 - N3	111.5	111.4	111.3	111.3
C4 - N3 - C2	105.6	105.5	105.3	105.4
N3 - C2 - C1	110.5	110.3	110.6	109.8
C2 - C1 - N5	104.6	104.9	106.0	106.3
C1 - N5 - C4	107.9	108.1	106.9	107.2
N9 - C8 - C1 - N5	180.0	179.9	175.9	-
C7 - N6 - C2 - N3	180.0	180.0	173.8	-
C1 - N5 - C12 - C13	-	-	-171.7	-

Table 3. *Calculated and experimental chemical shifts (with respect to TMS, all values in ppm) for N,1-dimethyl-4-(methylamino)-1H-imidazole-5-carboxamide (1, Caffeidine).*

atom	Relative chemical shifts HF/6-31G(d)	Difference	Relative chemical shifts HF/6-311G(d)	Difference	Relative chemical shifts HF/6-311+G(2d,p)	Difference	Experimental shifts
C1	96,56	-8,99	100,83	4,72	102,85	2,70	105,55
C2	165,72	10,50	168,34	-13,12	173,13	-17,91	155,22
C4	152,95	14,70	150,51	-12,26	152,32	-14,07	138,25
C7	27,64	-2,31	26,62	3,33	21,93	8,02	29,95
C8	176,85	11,16	173,63	-7,94	175,54	-9,85	165,69
C10	30,51	4,66	27,56	-1,71	22,78	3,07	25,85
C12	30,93	-4,81	30,46	5,28	22,74	13,00	35,74
H13	7,72	-0,13	6,93	0,92	8,13	-0,28	7,85
H14	5,48		3,64		4,57		
H15	2,78	-0,13	2,43	0,48	3,81	-0,90	2,91
H16	2,92	0,01	3,04	-0,13	3,07	-0,16	2,91
H17	2,39	-0,52	2,29	0,62	3,13	-0,22	2,91
H18	3,32		2,32		3,68		
H19	2,66	-0,22	2,28	0,60	3,46	-0,58	2,88
H20	2,57	-0,31	2,27	0,61	3,30	-0,42	2,88
H21	2,68	-0,20	2,47	0,41	3,17	-0,29	2,88
H22	3,63	-0,27	2,79	1,11	4,31	-0,41	3,9
H23	3,26	-0,64	3,36	0,54	4,38	-0,48	3,9
H24	3,25	-0,65	2,93	0,97	4,15	-0,25	3,9
atom	Relative chemical shifts B3LYP/6-31G(d)	Difference	Relative chemical shifts B3LYP /6-311G(d)	Difference	Relative chemical shifts B3LYP /6-311G(d)	Difference	Experimental shifts
C1	99,29	6,26	108,95	-3,40	109,32	-3,77	105,55
C2	151,76	3,46	168,34	-13,12	168,31	-13,09	155,22
C4	134,16	4,09	146,11	-7,86	147,42	-9,17	138,25
C7	28,47	1,48	30,07	-0,12	28,98	0,97	29,95
C8	159,80	5,89	175,21	-9,52	176,17	-10,48	165,69
C10	31,73	-5,88	33,46	-7,61	32,94	-7,09	25,85
C12	31,94	3,80	33,19	2,55	32,94	2,80	35,74
H13	6,73	1,12	6,93	0,92	7,25	0,60	7,85
H14	5,35		5,57		6,36		
H15	2,78	0,13	2,98	-0,07	3,00	-0,09	2,91
H16	2,90	0,01	3,11	-0,20	3,18	-0,27	2,91
H17	2,22	0,69	2,51	0,40	2,57	0,34	2,91
H18	3,18		3,44		3,76		
H19	2,62	0,26	2,81	0,07	2,80	0,08	2,88
H20	2,58	0,30	2,77	0,11	2,77	0,11	2,88
H21	2,71	0,17	2,81	0,07	2,85	0,03	2,88
H22	3,58	0,32	3,72	0,18	3,81	0,09	3,9
H23	3,20	0,70	3,35	0,55	3,51	0,39	3,9
H24	3,15	0,75	3,29	0,61	3,40	0,50	3,9

Table 4. *Calculated and experimental chemical shifts (with respect to TMS, all values in ppm) for N-methyl-4-(methyl-amino)-1H-imidazole-5-carboxamide (2, Theophyllidine)*

atom	Relative chemical shifts HF/6-31G(d)	Difference	Relative chemical shifts HF/6-311G(d)	Difference	Relative chemical shifts HF/6-311+G(2d,p)	Difference	Experimental shifts
C1	102,92	-10,48	108,03	-5,37	97,27	-16,13	113,4
C2	173,76	25,41	183,90	35,55	174,53	26,18	145,35
C4	150,55	21,68	157,95	29,08	148,88	20,01	128,87
C7	31,54	1,73	32,63	2,82	21,68	-8,13	29,81
C8	172,62	10,58	181,55	19,51	172,04	10,00	162,04
C11	32,33	6,74	32,80	7,21	22,14	-3,45	25,59
H12	8,40	0,18	8,34	0,12	8,26	0,04	8,22
H13	7,11	7,11	7,27	7,27	7,60	7,60	8,3
H14	4,89	0,11	5,11	0,33	5,42	0,64	4,78
H15	4,13	1,20	4,30	1,37	3,94	1,01	2,93
H16	3,33	0,40	3,54	0,61	3,18	0,25	2,93
H17	3,31	0,38	3,53	0,60	3,20	0,27	2,93
H18	3,39	3,39	3,58	3,58	3,71	3,71	4,87
H19	3,70	0,86	3,82	0,98	3,62	0,78	2,84
H20	3,53	0,69	3,63	0,79	3,30	0,46	2,84
H21	3,39	0,55	3,51	0,67	3,24	0,40	2,84
atom	Relative chemical shifts B3LYP/6-31G(d)	Difference	Relative chemical shifts B3LYP /6-311G(d)	Difference	Relative chemical shifts B3LYP/6-311+G(2d,p)	Difference	Experimental shifts
C1	103,49	9,91	113,23	0,17	113,20	0,20	113,4
C2	159,60	-14,25	176,20	-30,85	177,12	-31,77	145,35
C4	131,52	-2,65	143,22	-14,35	144,99	-16,12	128,87
C7	33,18	-3,37	35,30	-5,49	34,32	-4,51	29,81
C8	156,94	5,10	172,31	-10,27	173,50	-11,46	162,04
C11	33,83	-8,24	35,64	-10,05	35,09	-9,50	25,59
H12	7,34	-2,56	7,52	0,70	7,96	0,26	8,22
H13	7,02	-4,09	7,31	0,99	7,99	0,31	8,3
H14	4,86	-1,93	5,07	-0,29	5,81	-1,03	4,78
H15	4,04	-1,11	4,27	-1,34	4,34	-1,41	2,93
H16	3,13	-0,20	3,47	-0,54	3,49	-0,56	2,93
H17	3,41	-0,48	3,64	-0,71	3,65	-0,72	2,93
H18	3,19	1,68	3,44	1,43	3,95	0,92	4,87
H19	3,79	-0,95	3,92	-1,08	4,06	-1,22	2,84
H20	3,40	-0,56	3,61	-0,77	3,67	-0,83	2,84
H21	3,47	-0,63	3,68	-0,84	3,78	-0,94	2,84

Table 5. *Calculated and experimental chemical shifts (with respect to TMS, all values in ppm) for 1-(2-hydroxyethyl)-N-methyl-4-(methylamino)-1H-imidazole-5-carboxamide (3, Etofyllidine)*

atom	Relative chemical shifts HF/6-31G(d)	Difference	Relative chemical shifts HF/6-311G(d)	Difference	Relative chemical shifts HF/6-311+G(2d,p)	Difference	Experimental shifts
C1	106,65	2,13	110,90	6,38	102,69	-1,83	104,52
C2	171,77	10,26	164,56	3,05	172,32	10,81	161,51
C4	155,20	23,45	141,87	10,12	153,02	21,27	131,75
C7	31,78	1,69	38,28	8,19	21,96	-8,13	30,09
C8	176,52	3,25	164,90	-8,37	176,15	2,88	173,27
C10	31,97	6,13	38,46	12,62	21,69	-4,15	25,84
C12	46,08	-4,87	55,71	4,76	38,06	-12,89	50,95
C13	61,42	1,72	71,94	12,24	53,34	-6,36	59,7
H15	8,34	-0,05	7,68	-0,71	8,20	-0,19	8,39
H16	3,72		4,12		4,21		
H17	3,23	0,30	3,73	0,80	3,12	0,19	2,93
H18	3,96	1,03	4,25	1,32	3,76	0,83	2,93
H19	3,20	0,27	3,41	0,48	3,05	0,12	2,93
H20	3,57		3,85			3,83	
H21	3,59	0,71	4,03	1,15	3,30	0,42	2,88
H22	3,72	0,84	4,13	1,25	3,54	0,66	2,88
H23	3,40	0,52	3,75	0,87	3,14	0,26	2,88
H24	4,62	0,17	4,87	0,42	4,40	-0,05	4,45
H25	4,92	0,47	5,29	0,84	4,62	0,17	4,45
H26	4,30	0,42	4,99	1,11	3,99	0,11	3,88
H27	3,82	-0,06	4,57	0,69	3,55	-0,33	3,88
H28	0,60	0,60	0,44	0,44	0,36	0,36	
atom	Relative chemical shifts B3LYP/6-31G(d)	Difference	Relative chemical shifts B3LYP /6-311G(d)	Difference	Relative chemical shifts B3LYP/6-311+G(2d,p)	Difference	Experimental shifts
C1	106,09	1,57	116,51	11,99	118,99	14,47	104,52
C2	159,75	-1,76	176,62	15,11	178,70	17,19	161,51
C4	137,06	5,31	148,37	16,62	151,47	19,72	131,75
C7	33,47	3,38	35,68	5,59	36,45	6,36	30,09
C8	160,70	-12,57	176,41	3,14	179,18	5,91	173,27
C10	33,65	7,81	35,42	9,58	36,51	10,67	25,84
C12	50,90	-0,05	54,78	3,83	56,30	5,35	50,95
C13	67,13	7,43	73,53	13,83	73,99	14,29	59,7
H15	7,28	-1,11	7,47	-0,92	8,24	-0,15	8,39
H16	3,73		3,90		4,95		
H17	3,33	0,40	3,55	0,62	3,98	1,05	2,93
H18	3,86	0,93	4,09	1,16	4,55	1,62	2,93
H19	3,01	0,08	3,35	0,42	3,78	0,85	2,93
H20	3,46		3,73		4,55		

atom	Relative chemical shifts B3LYP/6-31G(d)	Difference	Relative chemical shifts B3LYP /6-311G(d)	Difference	Relative chemical shifts B3LYP/6-311+G(2d,p)	Difference	Experimental shifts
H21	3,63	0,75	3,85	0,97	4,21	1,33	2,88
H22	3,74	0,86	3,88	1,00	4,29	1,41	2,88
H23	3,35	0,47	3,57	0,69	3,99	1,11	2,88
H24	4,48	0,03	4,70	0,25	5,17	0,72	4,45
H25	4,89	0,44	5,12	0,67	5,49	1,04	4,45
H26	4,59	0,71	4,72	0,84	5,08	1,20	3,88
H27	4,18	0,30	4,30	0,42	4,70	0,82	3,88
H28	0,05		0,32		0,62		

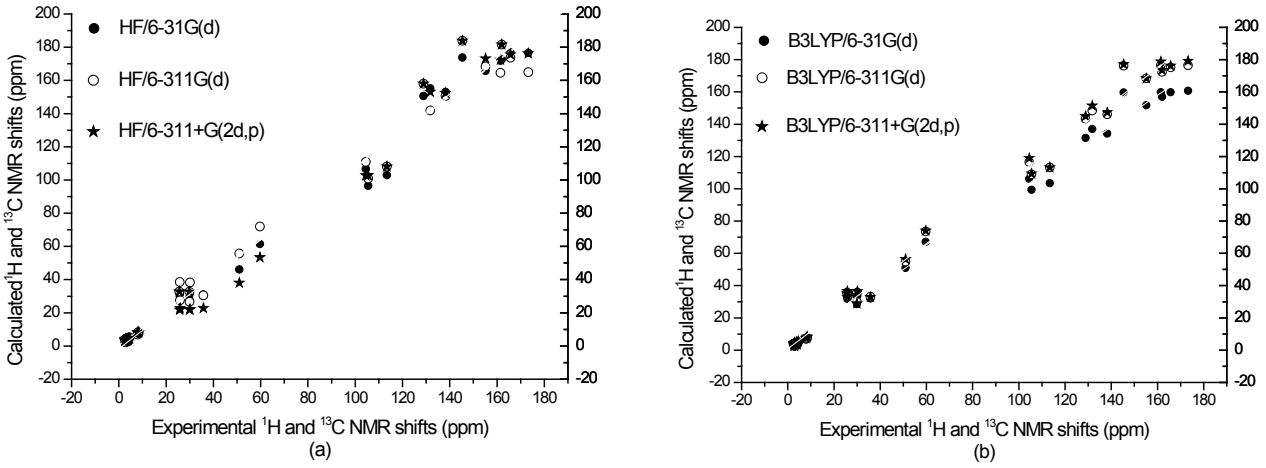

Fig. 2. *Plot of overall 1H- and 13C-NMR data for HF (a) and DFT (b) calculations.*

Table. 6. *Linear regression between overall experimental chemical shifts and calculated values, $\delta_{calc} = a + b\delta_{exp}$ (r – Pearson correlation coefficient, r^2 – coefficient of determination (COD), RMSE – root mean square error)*

Parameter	HF			DFT		
	6-31G (d)	6-311G (d)	6-311+G (2d,p)	6-31G (d)	6-311G (d)	6-311+G (2d,p)
a	-0.40	0.40	-1.67	0.99	0.67	0.78
b	1.07	1.07	1.09	0.98	1.08	1.09
r	0.9957	0.9936	0.9932	0.9974	0.9975	0.9974
r^2	0.9915	0.9872	0.9864	0.9948	0.9949	0.9948
RMSE	5.91	7.24	7.64	4.22	4.57	4.67

As seen from the presented results the values of the determined RMSE are between 4.22 ppm and 7.64 ppm for the different basis sets. These values also indicate that 6-31G(d) basis set provides better fit for all chemical shifts both at HF calculations (5.91 ppm) and DFT calculations (4.22 ppm). For overall chemical shifts determined in this study was observed, that the B3LYP/6-31G(d) calculations gave more satisfactory results.

This relationship is also shown in the results for the individual compounds in which the value of COD is above 0.9872. (Table 7).

A linear correlation between theoretical and experimental ^{13}C and ^{1}H chemical shifts is clearly visible in Tables 8 – 9. The sequence of 13C isotropic shielding constants was helpful in the spectra assignment. As one can easily see from linear correlation coefficients in Table 8, the experimental shifts for carbons are in better agreement with the HF/6-311 G(d) and B3LYP/6-31 G(d). Among the individual carbon atoms the large average differences were found at the C2 and C4 carbons in the imidazole. It can be seen that the chemical shifts of the cited carbon atoms are not well produced by all basis sets. This is probably due to sensitivity of the calculations to geometry and rapid rotation of the groups, particularly at the NMR time scale.

A linear correlation between theoretical and experimental 13C and 1H chemical shifts is clearly visible in Tables 8 – 9. The sequence of 13C isotropic shielding constants was helpful in the spectra assignment. As one can easily see from linear correlation coefficients in Table 8, the experimental shifts for carbons are in better agreement with the HF/6-311 G(d) and B3LYP/6-31 G(d). Among the individual carbon atoms the large average differences were found at the C2 and C4 carbons in the imidazole. It can be seen that the chemical shifts of the cited carbon atoms are not well produced by all basis sets. This is probably due to sensitivity of the calculations to geometry and rapid rotation of the groups, particularly at the NMR time scale.

As presented in Table 9, there is a good agreement between the experimental and theoretical 1H chemical shift results for the tested compounds. It was seen, that in both approaches, the larger basis sets gave more reliable results. As expected the values of the obtained results from HF method with larger basis sets are bigger than the ones calculated with the DFT methods with the same basis sets, due to the deficiency of electron correlation.

Table. 7. *Linear regression between overall experimental chemical shifts and calculated isotropic shielding constants (ppm)* $\boldsymbol{\delta_{calc} = a + b\delta_{exp}}$ *(r – Pearson correlation coefficient,* r^2 *– coefficient of determination (COD), RMSE – root mean square error)*

Comp	Parameter	HF			DFT		
		6-31G (d)	6-311G (d)	6-311+G (2d,p)	6-31G (d)	6-311G (d)	6-311+G (2d,p)
1	a	-1.27	0.40	-1.67	-0.07	0.67	0.78
	b	1.06	1.07	1.10	0.97	1.08	1.09
	r	**0.9974**	0.9936	0.9932	**0.9994**	0.9975	0.9974
	r^2	**0.9948**	0.9872	0.9864	**0.9988**	0.9949	0.9948
	RMSE	4.72	7.24	7.63	2.08	4.57	4.67
2	a	0.15	0.40	-1.67	1.30	0.67	0.78
	b	1.10	1.07	1.10	1.00	1.08	1.09
	r	0.9936	0.9932	0.9932	0.9975	0.9959	0.9974
	r^2	**0.9872**	0.9864	0.9864	**0.9949**	0.9918	0.9948
	RMSE	**7.24**	8.52	7.64	**4.57**	6.00	4.66
3	a	0.08	0.40	-1.67	1.78	0.66	0.78
	b	1.06	1.07	1.10	0.98	1.08	1.09
	r	0.9971	0.9936	0.9932	0.9976	0.9975	0.9974
	r^2	**0.9941**	0.9872	0.9864	**0.9952**	0.9949	0.9948
	RMSE	**4.84**	7.24	7.63	**4.03**	4.57	4.69

Table. 8.*Linear regression between experimental and calculated 13C chemical shifts (ppm)* $\delta_{calc} = a + b\delta_{exp}$
(r – Pearson correlation coefficient, r^2 – coefficient of determination (COD), RMSE – root mean square error)

Comp.	Parameter	HF			DFT		
		6-31G(d)	6-311G(d)	6-311+ G(2d,p)	6-31G(d)	6-311G(d)	6-311+ G(2d,p)
1	a	-4.98	-6.11	-13.58	1.23	-0.52	1.42
	b	1.09	1.10	1.17	0.96	1.08	1.08
	r	0.9946	**0.9972**	0.9971	**0.9986**	0.9984	0.9985
	r^2	0.9892	**0.9943**	0.9942	**0.9972**	0.9968	0.9971
	RMSE	7.76	**5.65**	6.05	**3.48**	4.11	3.97
2	a	0.42	-1.61	-1.61	5.566	4.52	3.31
	b	1.10	1.17	1.17	0.97	1.07	1.09
	r	0.9814	**0.9816**	0.9814	**0.9990**	0.9885	0.9884
	r^2	0.9631	**0.9636**	0.9631	**0.9781**	0.9771	0.9770
	RMSE	15.10	**14.10**	15.10	**9.53**	10.81	11.0
3	a	-.050	13.50	-12.50	8.58	7.99	8.53
	b	1.06	0.92	1.14	0.92	1.02	1.03
	r	0.9928	**0.9959**	0.9934	**0.9962**	0.9964	0.9965
	r^2	0.9857	**0.9919**	0.9869	**0.9924**	0.9928	0.9930
	RMSE	8.13	**5.28**	8.30	**5.12**	5.51	5.52

Table. 9.*Linear regression between experimental and calculated 1H chemical shifts (ppm)* $\delta_{calc} = a + b\delta_{exp}$
(r – Pearson correlation coefficient, r2 – coefficient of determination (COD), RMSE – root mean square error)

Comp.	Parameter	HF			DFT		
		6-31G(d)	6-311G(d)	6-311+ G(2d,p)	6-31G(d)	6-311G(d)	6-311+ G(2d,p)
1	a	-0.35	-0.21	0.51	0.21	0.40	0.26
	b	1.01	0.89	0.97	0.82	0.82	0.88
	r	0.9897	0.9761	0.9899	0.9852	0.9862	0.9891
	$\underline{r}^2$	0.9795	0.9528	0.9799	0.9706	0.9726	0.9782
	RMSE	0.24	0.32	0.23	0.23	0.22	0.21
2	a	0.96	1.22	0.79	1.49	1.74	1.59
	b	089	0.85	0.92	0.71	0.70	0.79
	r	0.9815	0.9869	0.9880	0.980	0.9784	0.9842
	r^2	0.9705	0.9741	0.9761	0.9602	0.9572	0.9686
	RMSE	0.32	0.30	0.28	0.30	0.34	0.26
3	a	0.91	1.92	0.66	1.52	1.75	1.96
	b	0.87	0.70	0.88	0.70	0.69	0.75
	r	0.9816	0.9814	0.9718	0.9716	0.9772	0.9835
	r^2	0.9444	0.9631	0.9636	0.9439	0.9550	0.9673
	RMSE	0.29	0.29	0.29	0.29	0.26	0.24

In this study, the differences in the performance of used basis sets are almost negligible for the performed analysis of protons. The root mean square values given in Table 9 indicate that the 6-311+G(d,p) basis set provides better fit for chemical shifts than the other basis sets. The obtained b values differ statistically significant from zero ($P < 0.001$), which means that the linear model used is adequate and correctly describes the dependence between the experimental and the calculated values of the corresponding chemical shifts.

Antiprolipherative activity

The antiproliferative and cytotoxic activity of the investigated compounds was evaluated using a standard MTT assay after 72 hours of exposure on human tumor cell lines BV-173 (chronic myelogenous leukemia) and KG-1 (acute myeloid leukemia). Clinically applied alkylating cytostatic melphalan was used as a positive control. The data obtained were fitted to concentration – effect sigmoid curves and the corresponding IC_{50} values were calculated, using a non-linear regression analysis.

The studied compounds demonstrated pronounced, concentration dependent anti-proliferative activity, whereas at the highest concentrations used resulted in complete elimination of the malignant cell population, which proves cytotoxic activity. The resulting concentration effect dependencies are presented in Fig. 3, and the calculated IC50 values are summarized in Table 10.

The analysis of the obtained data shows that the established anti-proliferative activity of the newly synthesized imidazole derivatives may be arranged in the following increasing order: 1 <2 <3.

Based on the established ability to inhibit proliferation and tumor cells vitality, the tested compounds may be recognized as leading structures for future development of new anti-neoplastic agents.

Table 10. *IC_{50} values of tested compounds and of referent cytostatic Melphalan*

Compounds	IC_{50} values (μmol/L)	
	BV-173	KG-1
1	214.1 ± 9.9	128.8 ± 6.7
2	161.4 ± 7.8	129.9 ± 4.9
3	107.9 ± 6.9	115.1 ± 3.0
Melphalan	25.4 ± 1.9	21.9 ± 1.7

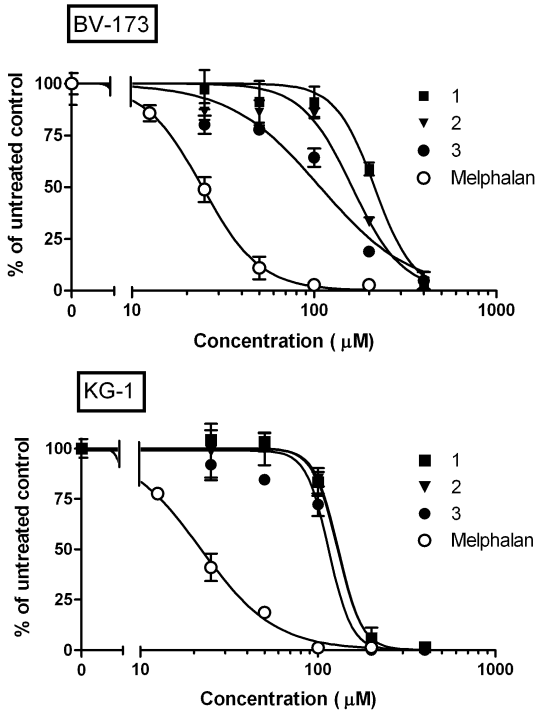

Fig. 3. *Antiproliferative effects of tested compounds on the human tumor cell lines after 72 hours of incubation (MTT assay).*

Conclusion

Correlations between experimental chemical shifts and GIAO-calculated isotropic shielding constants of hydrogens and carbons was obtained for a series of imidazole derivatives, in order to assess the performance of NMR spectral calculations using both HF and DFT-B3LYP level of theory with different basis sets. The 6-31G (d), 6-311G (d) and 6-311+G (d,p) basis sets were considered for geometry optimization and spectral calculations.

It was determined, that the experimental shifts for carbons are in better agreement with the HF/6-311 G(d) and B3LYP/6-31 G(d) calculations. For protons it is clear that the 6-311+G(d,p) basis set provides better fit for chemical shifts than the other basis sets (rmse = 0.27 ± 0.02 ppm for HF calculation and 0.024 ± 0.03 ppm for DFT calculation). The obtained b values differ statistically significant from zero ($P < 0.001$), which means that the linear model used is adequate and correctly describes the dependence between the experimental and the calculated values of the corresponding chemical shifts.

The analysis of the obtained data for antiproliferative activity shows that the newly synthesized imidazole derivatives possess this kind of activity and they can be recognized as the leading structures for development of new anti-neoplastic agents.

References

1. Grimment, MR. Imidazoles and their Benzo Derivatives. In: Katritzky AR and Rees C W (eds.). Comprehensive Hetereocyclic Chemistry, Oxford, Pergamon: 1984, Vol. 5, pp. 457–498.
2. Mavrova A, Anichina K, Vuchev D, Tsenov J, Denkova P, Kondeva M, Micheva M. Anthelminthic activity of some newly synthesized 5(6)-(un)substituted-1H-benzimidazol-2-ylthioacetylpiperazine derivatives. Eur. J. Med. Chem., 2006; 41(12): 1412–1420.
3. Sheng J, Nguyen P, Baldeck J, Olsson J, Marquis R. Antimicrobial actions of benzimidazoles against the oral anaerobes Fusobacterium nucleatum and Prevotella intermedia. Arch. Oral Biol., 2006; 51(11): 1015-1023.
4. Uçucu Ü, Karaburun N, Işikdağ İ. Synthesis and analgesic activity of some 1-benzyl-2-substituted-4,5-diphenyl-1H-imidazole derivatives. Il Farmaco, 2001; 56 (4): 285-290.
5. Uto Y, Nagasawa H,. Jin C-Z, Nakayama S, Tanaka A, Kiyoi S, Nakashima H, Shimamura M, Inayama S, Fujiwara T, Takeuchi Y, Uehara Y, Kirk KL, Nakata E, Hor H. Design of antiangiogenic hypoxic cell radiosensitizers: 2-Nitroimidazoles containing a 2-aminomethylene-4-cyclopentene-1,3-dione moiety. Bioorganic & Medicinal Chemistry, 2008; 16 (11): 6042-6053,
6. Mulcahy R, Gipp J, Carminati A, Barascut J-L, Imbach J-L. Chemosensitization at reduced nitroimidazole concentrations by mixed-function compounds combining 2-nitroimidazole and chloroethylnitrosourea. European Journal of Cancer and Clinical Oncology, 1989; 25 (7): 1099-1104.
7. Brown AM, Hoopes SL, White RH, Sarisky CA. Purine biosynthesis in archaea: variations on a theme. Biology Direct, 2011; 6:63. http://www.biology-direct.com/content/6/1/63.
8. Ashihara H, Sano H, Crozier A. Cafeine and related purine alkaloids: Biosynthesis, catabolism, function and genetic engineering. Phytochemistry, 2008; 69(4): 841–856.
9. Auterhoff H, Hebler M, Theophyllidine, its preparation and characterization, Arzneimittelforschung, 1959; 9: 621-2.
10. Ivankovic S, Seibel J, Komitowski D, Spiegelhalder B, Preussmann R, Siddiqi M, Caffeine-derived N-nitroso compounds. V. Carcinogenicity of mononitrosocaffeidine and dinitrosocaffeidine in bd-ix rats, Carcinogenesis, 1998; 19(5): 933-937.
11. Kumar R, Wacker C-D, Mende P, Spiegelhalder B, Preussmann R, Siddiqi M, Caffeine-derived N-nitroso compounds. II. Synthesis and characterisation of nitrosation products from caffeidine and caffeidine acid. Chem. Res. Toxicol., 1993; 6(1): 50-58.
12. Ali Jalili M, Navidrouyan M, A new method for synthesis of Theophilidine and its derivatives, Int. J. Adv. Pharm. Sci., 2010; 1: 172-175
13. Schleyer PVR, Allinger NL; Clark T; Gasteiger J; Kolmann PA; Schaefer HF; Schreiner PR, The encyclopedia of computational chemistry; John Wiley & Sons, Chichester: 1998.
14. Ferraro MB. B3LYP density functional calculations of 1H and 13C nuclear shielding constants of some unsymmetric N, N0-dipyridyl ureas and a further insight into their molecular conformations. J. Mol. Struc. (Theochem), 2000; 528(1-3): 199–209
15. Ditchfield R. Self-consistent perturbation theory of diamagnetism. I A gauge-invariant LCAO method for N.M.R. chemical shifts. Mol. Phys., 1974; 27: 789-807.
16. Buhl M, Gauss J, Hofmann M, Schleyer PvR. Decisive electron correlation effects on computed boron-11 and carbon-13 NMR chemical shifts. Application of the GIAO-MP2 method to boranes and carbaboranes. J. Amer. Chem. Soc., 1993; 115(26): 12385-12390.
17. CambridgeSoft 2008, ver. 11.0.1
18. Frisch A, Nielsen AB, Holder AJ, Pittsburg MJ, Frisch GW, Trucks HB et al., Gaussian 03W Revision D.01 Version 6.1, Gaussian Inc, Pittsburgh, PA (2003).
19. GaussView, Version 3, Roy Dennington, Todd Keith and John Millam, Semichem Inc., Shawnee Mission KS, 2003.
20. Dewar MJS, Zoebisch EG, Healy EF, Stewart JJP. Development and use of quantum mechanical molecular models. 76. AM1: A new general purpose quantum mechanical molecular model. J. Amer. Chem. Soc., 1985, 107(13): 3902-3909.
21. Avci D, Atalay Y. Effects of different GIAO and CSGT models and basis sets on 2-aryl-1,3,4-oxadiazole derivatives. Struct Chem (2009) 20:185–201.

22. Womacott T.M., Womacott R.J., Introductory Statistics, fifth ed., Wiley, New York, 1990.

23. Mosmann T. Rapid colorimetric assay for cellular growth and survival: application to proliferation and cytotoxicity assays. J Immunol Methods. 1983;65(1-2):55-63.

24. Konstantinov SM, Eibl H, Berger MR. BCR-ABL influences the antileukaemic efficacy of alkylphosphocholines. Br J Haematol. 1999;107(2):365-80.

25. Martinez-Carrera S. The crystal structure of imidazole at -150°C. Acta Cryst., 1966, 20(6): 783-789

26. Poltev VI, Grokhina TI, González E, Deriabina A, Cruz A, Gorb L, Leszczynski J, Djimant LN, Veselkov A. The study of three-dimentional structure of caffeine associates using computational and experimental methods. J. Molec. Structure (Theochem), 2004, 709(1-3): 123-128.

27. Egawa T, Kamiya A, Takeuchi H, Konaka S. Molecular structure of caffeine as determined by gas electron diffraction aided by theoretical calculations, J. Mol. Struct., 2006, 825(1-3): 151-157.

✉ **Corresponding author**
Maya Georgieva
Faculty of pharmacy, Medical University, Sofia
2 "Dunav" str., 1000 Sofia, Bulgaria
phone: +359 2 9236 515;
e-mail: georgm@mail.bg